8264 *Macromolecules* **2010**, *43*, 8264–8274
DOI: 10.1021/ma1012495

Macromolecules
ARTICLE

Complexation of siRNA with Dendrimer: A Molecular Modeling Approach

V. Vasumathi* and Prabal K. Maiti*

Centre for Condensed Matter Theory, Department of Physics, Indian Institute of Science, Bangalore-560012, India

Received June 4, 2010; Revised Manuscript Received August 19, 2010

ABSTRACT: This paper reports the structural behavior and thermodynamics of the complexation of siRNA with poly(amidoamine) (PAMAM) dendrimers of generation 3 (G3) and 4 (G4) through fully atomistic molecular dynamics (MD) simulations accompanied by free energy calculations and inherent structure determination. We have also done simulation with one siRNA and two dendrimers (2×G3 or 2×G4) to get the microscopic picture of various binding modes. Our simulation results reveal the formation of stable siRNA−dendrimer complex over nanosecond time scale. With the increase in dendrimer generation, the charge ratio increases and hence the binding energy between siRNA and dendrimer also increases in accordance with available experimental measurements. Calculated radial distribution functions of amines groups of various subgenerations in a given generation of dendrimer and phosphate in backbone of siRNA reveals that one dendrimer of generation 4 shows better binding with siRNA almost wrapping the dendrimer when compared to the binding with lower generation dendrimer like G3. In contrast, two dendrimers of generation 4 show binding without siRNA wrapping the dendrimer because of repulsion between two dendrimers. The counterion distribution around the complex and the water molecules in the hydration shell of siRNA give microscopic picture of the binding dynamics. We see a clear correlation between water, counterions motions and the complexation i.e. the water molecules and counterions which condensed around siRNA are moved away from the siRNA backbone when dendrimer start binding to the siRNA backbone. As siRNA wraps/bind to the dendrimer counterions originally condensed onto siRNA (Na^+) and dendrimer (Cl^-) get released. We give a quantitative estimate of the entropy of counterions and show that there is gain in entropy due to counterions release during the complexation. Furthermore, the free energy of complexation of 1G3 and 1G4 at two different salt concentrations shows that increase in salt concentration leads to the weakening of the binding affinity of siRNA and dendrimer.

I. Introduction

RNA interference (RNAi) is a regulatory mechanism by which eukaryotic cells use small double stranded RNA (dsRNA) molecules to control expression of pathogenic gene or over-expression of gene activity.[1,2] RNA interference (RNAi) was discovered by Fire and Mello when they found that they can silence target genes in *Caenorhabditis elegans* (*C. elegans*) by delivering long, double-stranded RNAs (dsRNAs).[3] Briefly the RNAi mechanism can be described as follows:[1] First, the long, double-stranded RNAs (either delivered to cells or expressed intracellularly from plasmids) are processed into short 21−25 base pair (bp) fragments by an RNase III type enzyme called Dicer. These small double stranded RNA (dsRNA) molecules are known as small interfering RNAs (siRNA). siRNA has 2-nucleotide 3′-overhangs at both ends (2 unpaired nucleotides) which helps them to be recognized by enzyme for further processing. Then, each siRNA is loaded into an RNA-induced silencing complex (RISC). Depending on the directionality of siRNA loading, Ago2, an enzyme component of RISC, cleaves and discards one strand (passenger) and retains the other (guide) to activate the mature RISC complex.[1] The siRNA guide strand then directs RISC to mRNA molecules containing a complementary sequence. Through Watson−Crick base pairing, the siRNA strand binds to the complementary portion of the mRNA molecule and the endonuclease region of RISC cleaves the mRNA in this region of homology.[4] The cleaved mRNA, which is subsequently degraded by intracellular nucleases, is no longer available for translation into protein.[5] It is through this mechanism that long dsRNAs are able to induce gene silencing with very high specificity. Within a decade of the discovery of RNA interference (RNAi), it has emerged as an attractive route where affected gene can be silenced (gene silencing) by delivering siRNA to the disease cell.[6−8] Several major findings have indicated that RNAi mechanism can be exploited to control genes associated with many human disease such as cancer, autoimmune diseases, dominant genetic disorders and viral infections.[9−13] This has made RNAi an attractive choice for future therapeutics. There are instances of planned human clinical trial as well.

However, the major challenge faced by the siRNA-based therapy is its delivery/entry to the desired location (affected cell, tissue or other organs). Like DNA, siRNA is negatively charged and hence faces significant barrier for its entry to the cell membrane. Also the sizes of native siRNA make its transfection through the membrane very slow. It can also get degraded in serum. One remedy of this problem is the compaction of siRNA by the virus particle and then the complex can be delivered. However, viral based delivery of siRNA has similar problems as encountered in DNA delivery such as unpredictable immune response and slow transfection. This has prompted the development of other synthetic (nonviral) gene delivery systems.[14] Non-viral delivery systems generally consist of compaction of the

*Corresponding authors. E-mail: (V.V.) vasu@physics.iisc.ernet.in; (P.K.M.) maiti@physics.iisc.ernet.in.

 Published on Web 09/02/2010

Table 1. Details of the Simulation Condition of the siRNA−Dendrimer Complexes Studied in This Work

	total no. of atoms	no. of water molecules	Na^+ ions	Cl^- ions	[NaCl] (mM)	box volume (Å^3)	charge ratio (N/P)
1G3	82 876	26 760	44	32	0	836815	0.72
1G4	151 883	49 537	44	64	0	1575738	1.45
2G3	144 734	46 994	44	64	0	1525726	1.45
2G4	246 967	80 261	44	128	0	2523460	2.9
1G3	82 892	26 762	49	37	10	837625	0.72
1G3	83 412	26 890	117	105	150	841646	0.72
1G4	152 534	49 568	53	73	10	1583452	1.45
1G4	152 781	49 567	178	198	150	1582185	1.45

extended, negatively charged siRNA into a dense positively charged (or neutral) particle which can be transfected to the target cells via endocytosis.[15] RNA compaction can be achieved in various ways by using various nonviral delivery carriers such as linear or branched cationic polymers (dendrimer),[16−18] cationic lipids,[19−21] carbon nanotubes,[22−24] cell penetrating peptides,[25−27] and a few proteins.[28−30] Among these carrier, PAMAM dendrimer, is a new class of branched polymeric drug delivery vehicles which possess a well-defined, three-dimensional structure and a multivalent exterior that can be modified with surface groups.[31,32] Because of this dendritic architecture, multivalent polycationic surface group, the dendrimer offers a solution to potent drug delivery.[31] Several experiments indicates that lower toxicity and higher transfection efficiency can be obtained by using complexes between DNA and dendrimers[33−35] as well as for the complexes between siRNA and PAMAM dendrimers.[36−42] There exists several computational studies where complexation of a PAMAM dendrimer with oppositely charge model polyelectrolyte have been studied using all atom MD and coarse-grained MD as well Brownian dynamics simulations.[43−47] Earlier we reported a comprehensive study on the complexation of single stranded DNA (ssDNA) and PAMAM dendrimers of generation G2−G4.[48] It was shown that ssDNA coils around the PAMAM dendrimer of G4 generation where the positive overcharge on the dendrimer surface overcomes the bending rigidity of the DNA leading to a wrapping of the single-stranded DNA on the surface of the dendrimer. Although there exist several computational study of the complexation of DNA with dendrimer, study of dendrimer complexation with siRNA has just caught the attention of the community. In fact at the time of writing this article, a paper by Pavan et al.[49] reports the binding of GL3 siRNA with various generation PAMAM dendrimer and shows that G4 dendrimer has higher binding affinity than G5 and G6. However, the understanding of structure and dynamics of siRNA−dendrimer complex still remain very poor. Recent experimental studies suggest that G3 dendrimer can have better transfection efficiency for siRNA delivery when dendrimer is conjugate with α-cyclodextrin.[37] Further, the dynamic light scattering and fluorescence study on DNA complexes with several PAMAM dendrimers in dilute solution shows significant protection against DNase.[50] In this paper, we focused our attention on the structure of the complexation of siRNA with single G3 and G4 dendrimer. We also present results when more than one dendrimer is present during complexation. More specifically the present paper reports the complexation of siRNA with (i) one PAMAM dendrimer of generation 3 and 4, (ii) two dendrimers of same generations, and (iii) one dendrimer of same generations at two different salt concentrations. Our all atom molecular modeling studies give a quantitative estimate of the binding affinity of G3 and G4 dendrimer with siRNA and also provide microscopic understanding as to how the binding affinity and mechanism changes in going from one dendrimer to multidendrimer. We have also studied the nature of the complex at various salt concentrations to elucidate the role of electrostatic in the complexation process. The rest of the paper is organized as follows: in the next section we give the details of system preparation as well as simulation conditions. In section III, we discuss various results coming out from our all atom MD simulations and compare them with existing simulation/theoretical and experimental results where available. Finally in section IV we give a summary of the results and conclusions.

II. Simulation Details

MD simulations reported in this article used the PMEMD software package[51] with the all-atom AMBER03 force field (FF)[52] for siRNA and Dreiding FF[53] for the dendrimer. We have used molecular model of PAMAM dendrimers from our previous studies.[54] The initial structure of 21 base pairs siRNA was downloaded from Protein Data Bank (pdb code: 2F8S).[55] The dendrimer structure of a given generation was placed at the major groove of siRNA by using the LEAP module in AMBER. The resulting structures were then solvated in TIP3P water box, extending 17 Å (G3) and 20 Å (G4) from the solute in the three directions. Appropriate numbers of Na^+ and Cl^- counterions were added to neutralize the negative charges on the phosphate backbone of the siRNA structure and positive charges on the dendrimer amine sites, respectively. Above procedure resulted the siRNA−dendrimer complexes in a solvated form which contain siRNA, dendrimer (G3 or G4), water, Na^+ and Cl^- counterions. Thus, we have generated two 1:1 systems G3 + siRNA and G4 + siRNA. To study the effect of increasing charge ratio (N/P) for a given generation, we have also generated the complex system of siRNA with two dendrimers (e.g. 2×G3+siRNA for G3 and 2×G4 + siRNA for G4) by placing the second dendrimer on other side of siRNA using the LEAP module in AMBER . Again, the systems were solvated with a water box extending 20 Å (2G3) and 30 Å (2G4) from the solute in the case of 2G3 and 2G4 respectively. Here again some waters were replaced by Na^+ counterions to neutralize the negative charge on the phosphate groups of the backbone of the siRNA structures. Then appropriate numbers of Cl^- ions were added to neutralize the positive charges on the dendrimer amine sites. So far, we have prepared the system with neutral molarities. In order to mimic the experimental salt concentration and to study the effect of salt concentration on the complex formation, we have added 10 mM and 150 mM NaCl to 1:1 complex systems for both the G3 and G4 case. Since 2G3 and 2G4 systems sizes are very large, we didnot prepare the multidendrimer system in different salt concentration. We believe that the effect of salt concentration on 1:1 case is approximately similar to 2:1. Table 1 gives a summary of the simulation conditions reported in this paper.

Each resulting solvated structures were subjected to 1000 steps of steepest descent minimization of the potential energy, followed by 2000 steps of conjugate gradient minimization. During this minimization the siRNA and dendrimers were fixed in their starting conformations using harmonic constraints with a force constant of 500 kcal/mol/ Å^2. Because of the constraint on siRNA−dendrimer complexes, the water molecules reorganized themselves to eliminate bad contacts with the siRNA and dendrimers.

The minimized structures were then subjected to 40 ps of MD, using a 2 fs time step for integration. While doing the MD, the system

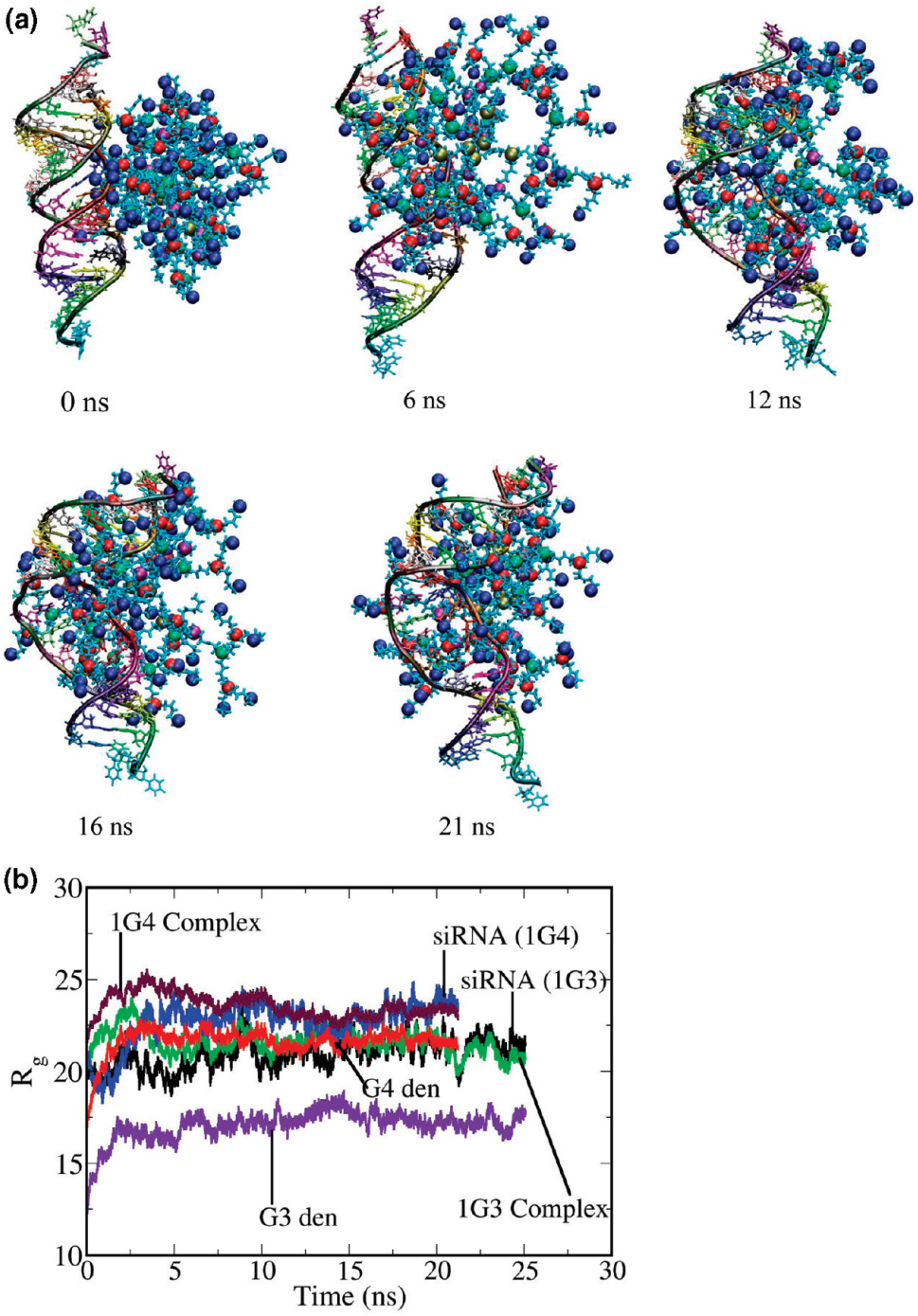

Figure 1. (a) Structure of siRNA−dendrimer complex for 1G4 case during various stages of the binding process at the interval of few ns. Amines of various subgenerations are shown in different colors. (b) Evolution of the size of the siRNA and dendrimer as well as of the complex showing the conformational change during the binding process.

was gradually heated from 0 to 300 K using weak 20 kcal/mol/ Å^2 harmonic constraints on the solute to its starting structure. This allows for slow relaxation of the built siRNA−dendrimer structures. In addition SHAKE constraints[56] using a geometrical tolerance of 5×10^{-4} Å were imposed on all covalent bonds involving hydrogen atoms. This is needed to prevent dynamically changes in the NH and OH bonds from disrupting associated hydrogen bonds. Subsequently, MD was performed under constant pressure−constant temperature conditions (*NPT*), with temperature regulation achieved using the Berendsen weak coupling method[57] (0.5 ps time constant for heat bath coupling and 0.2 ps pressure relaxation time). This was followed by another 5000 steps of conjugate gradient minimization while decreasing the force constant of the harmonic restraints from 20 (kcal/mol)/Å^2 to zero in steps of 5 kcal/(mol Å^2). The above-mentioned protocol produce very stable MD trajectory for such complex system and earlier was found to be adequate to study complexation of ssDNA with dendrimer as well as large DNA nanostructure in solution.[48,58] Finally, for analysis of structures and properties, we carried out 14−26 ns of NVT MD using a heat bath coupling time constant of 1 ps.

III. Results and Discussion

To characterize the complexation of siRNA with dendrimers we have calculated several kinetic and thermodynamics

quantities and classified them in the following two major categories:

1. Kinetics of complex formation
   a. Radius of gyration (R_g) of the complex as well as of siRNA and dendrimer in the complex
   b. Number of close contacts between siRNA and dendrimer.
   c. Na^+ counterion distributions around the siRNA.
   d. Number of water in the hydration shell of siRNA.
2. Binding Energy and Structural properties in equilibrium state
   a. Binding energy between dendrimer and siRNA using mm-pbsa and two phase thermodynamic model (2PT).
   b. Number of contacts between N and P
   c. Radial density distributions function between the phosphate of siRNA and amine of dendrimer.

III.1. Kinetics of Complex Formation. *III.1.1. Size of the Complex*. MD simulations reveal that it takes several nanoseconds for the siRNA to start wrapping around the dendrimer and in the next several nanoseconds (more than 15 ns) siRNA overcomes *several energetic and entropic bottlenecks* to find its optimal wrapping patterns on the dendrimer surface. In Figure 1a, we show several snapshots of the systems in a few ns interval to show the various stages in the siRNA binding process for the case of 1G4. Similar behavior is visible for other cases as well. *Note the significant conformational change of dendrimer and siRNA even after 16 ns*. The radius of gyration $\langle R_g \rangle$ provides a measure of the conformational change of siRNA as it binds and wraps around the dendrimer. We have also monitored the size of the dendrimer during the simulation. These results are shown in Figure 1b, which shows that the dendrimer *expands noticeably in the early stage* in order to optimize electrostatic interactions with the siRNA whose size also increases as binds to dendrimer. We find that the radius of gyration for siRNA or end-to-end length also increases. This causes the rise between the bases to increase which facilitate its binding to the dendrimer (see Figure S1 in the Supporting Information). Note that this is in sharp contrast to the DNA binding to the dendrimer where DNA length shortens as it binds to the dendrimer.

III.1.2. Number of Close Contacts. We have calculated the number of close contacts (within in the hydration shell of siRNA) between siRNA and dendrimer, by using the below formulas,

$$N_c(t) = \sum_{i=1}^{N_{siRNA}} \sum_{j=1}^{N_{Den}} \int_{r_i}^{r_i+3A^\circ} \delta(r(t) - r_j(t))\, \mathrm{d}r$$

Here, N_{siRNA} and N_{Den} are the total number of siRNA and dendrimer (G3 or G4 or 2xG3 or 2xG4) atoms, respectively, and r_j is the distance of j^{th} atom of dendrimer from i^{th} atom of siRNA. The delta function ensures counting of all dendrimer atoms within 3 Å from siRNA atoms. Figure 2a shows the number of close contacts (N_c) between the siRNA and dendrimer for various cases:

(i) complexation of siRNA with one dendrimer of generations 3 (G3) and generation 4 (G4);
(ii) complexation of siRNA with two dendrimers of generations 3 and generation 4.

The overall characteristic of all the graphs in the Figure 2a show almost oscillating and intermittent behavior. We observe the following interesting features from Figure 2a: for

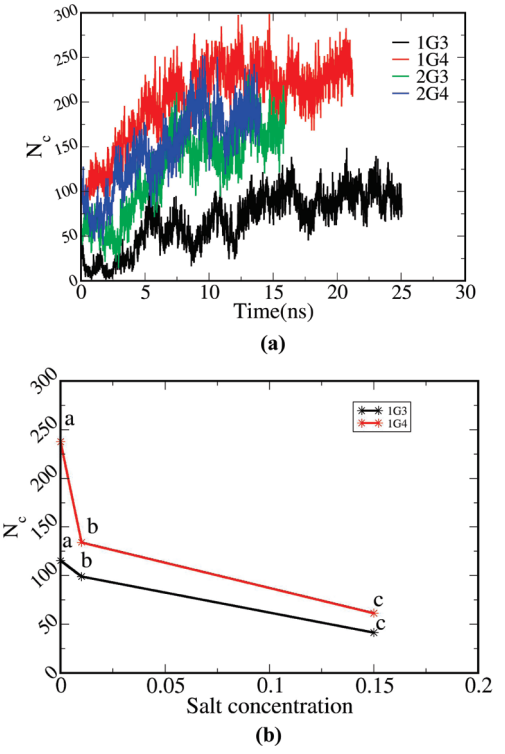

Figure 2. Variation of the number of close contact atoms between siRNA and dendrimer (any contact within in the hydration shell of siRNA) of (a) generation 3 (1G3) and 4 (1G4) and same generation with two dendrimers (2G3 and 2G4), (b) generation 3 and 4 at two different salt concentrations: here points a, b, and c correspond to 0, 10, and 150 mM NaCl concentrations. Lines are guides to the eye only.

one dendrimer case, the number of close contacts (N_c) is larger for G4 when compared to the case of G3. In general, the affinity for siRNA increases with increasing in dendrimer generation as the available surface area for binding increases with the increase of size with generation. Also the charge ratio between the siRNA and dendrimer increases with the increase in generation. Hence binding of dendrimer with siRNA is enhanced for G4 compared to G3. Next we consider the case of 1G4 and 2G3: size of G3 dendrimer is smaller when compared to the size of G4 dendrimer[54] so for the case of 2G3, two dendrimers are trying to bind siRNA in a way by moving themselves oppositely toward the ends of the siRNA and this way achieve better binding. Even though dendrimers are moving toward the two ends of siRNA, still there is a repulsion between these two dendrimers (see the snapshot given in Figure 3b). Because of this interdendrimer repulsion, we see the number of contacts for 1G4 case is higher than that of 2 G3 case. (N_c for 2G3 $<$ N_c for 1G4). Finally for the case of 1G4 and 2G4: here although the charge ratio is increased going from 1G4 to 2G4 the number of contacts N_c decreases because of the repulsion between the two dendrimers. Furthermore, for G4, the size of one dendrimer is large enough to almost wrap siRNA (see the snapshot given in Figure 3c). Because of this repulsion between two dendrimers, none of these two dendrimers are able to wrap siRNA; instead, it just binds or sticks to both sides of siRNA (see the snapshots given in Figure 3d). This can be compared to the case for G3 dendrimer. In going from 1G3 to 2G3, the number of contacts N_c between the dendrimer and siRNA is increased. Because of the small size of G3 dendrimer, single G3 cannot wrap the siRNA fully (see the structure in Figure 3a); instead, it wraps half of the siRNA. This is in contrast to the 2G3 case: two dendrimers

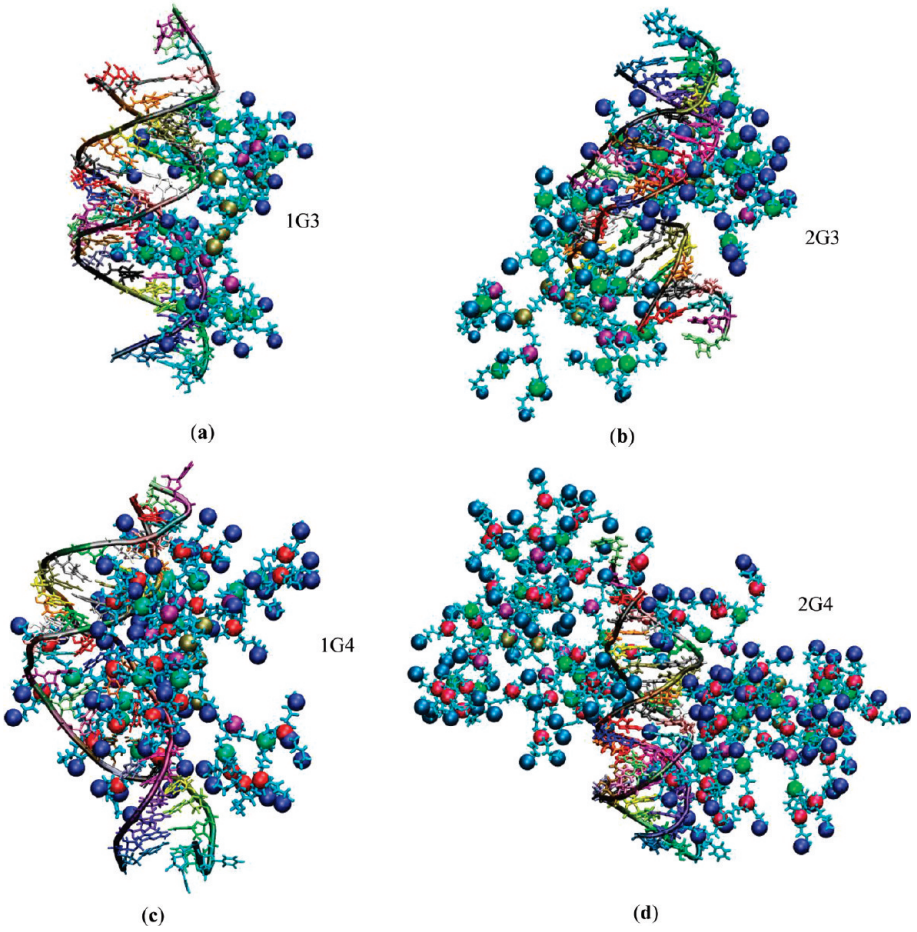

Figure 3. Structures of siRNA−dendrimer complexes: siRNA with (a) one dendrimer of generation 3 (1G3), (b) two dendrimers of generation 3(2G3), (c) one dendrimer of generation 4 (1G4), and (d) two dendrimers of generation 4 (2G4). Various amines are leveled different colored atoms say blue, green, purple, tyan correspond to terminal, 2nd, 1st, and core amines in G3 and blue, red, green, purple, tyan correspond to terminal, 3rd, 2nd, 1st, and core amines in G4.

moved away from each other to avoid maximum repulsion between them and then they try to wrap the siRNA (see the snapshot given in Figure 3b). Thus, the number of close contacts for 2G3 case is higher than that of 1G3 case, whereas the number of close contacts for 2G4 case is lower than that of 1G4 case. In Figure 2b we show the average number of close contacts for 1G3 and 1G4 at different salt concentrations. We find that as salt concentration increases the number of contacts N_c decreases because of the screening of the electrostatic interaction between siRNA and dendrimer at high salt concentration.

III.1.3. Counterion Distribution around the Complex. Previous theoretical and experimental works have demonstrated[59−66] that such complexation between two oppositely charged polyelectrolytes is also favored by the entropic gain due to counterion release.[67] But this has not been demonstrated from a microscopic all atom MD simulation, where it has been explicitly demonstrated that counterions do gain entropy when such complexation occurs. During the complexation of siRNA and dendrimer, the counterions moved away from the respective molecules. Initially Na^+ ions which are condensed around siRNA moved away from the siRNA molecule when dendrimer start binding. In order to see the above effect we have calculated the number of Na^+ counterions for all the cases and we plotted the time dependency of number of Na^+ ions in Figure 4. So far, we observe as the generation and concentration of dendrimer increases, the charge ratio increases and hence binding affinity gets increased.

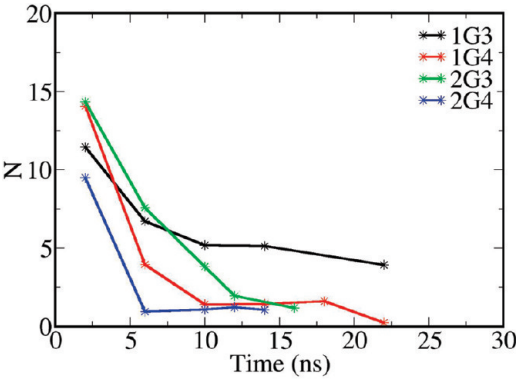

Figure 4. Time variation of the number (N) of Na^+ counterions around the siRNA (within 20 Å) of the all the cases. Lines are guides to the eye only.

Because of this higher generation of one dendrimer and two dendrimers cases show less number of Na^+ ions and also decreases rapidly which you can seen in Figure 4. From these results, one can say that depending upon the binding affinity the number of counters ions namely Na^+ (see Figure 4) are moved away from siRNA in other words for greater the binding affinity leads greater the number of ions are moved away from the molecules and vice versa.

Furthermore, we have calculated the entropy of the Na^+ ions which are in the spine of siRNA as well as when siRNA is in the complex state with dendrimer using 2PT methods.

Table 2. Entropy and Entropy Gain per Na^+ Counterion When siRNA Is Complexed with Dendrimer of Generation 3 and 4[a]

	1G3	1G4
entropy per Na^+ ion cal/(mol K)	9.5	9.8
entropy gain per Na^+ ion cal/(mol K)	0.5	0.8

[a] Here, for calculating entropy gain we have used the entropy per Na^+ counterion 9.0 cal/(mol K) (37.96 J/(mol K)) when only siRNA is present.

Table 3. Thermodynamic Parameters Determined by Molecular Dynamics along with MMPBSA and 2PT Methods for the Binding of (i) One Dendrimer of Generation 3 and 4 to siRNA, (ii) Two Dendrimers of the Same Generations to siRNA, and (iii) One Dendrimer of the Same Generations at Two Different Salt Concentrations

complex	ΔH (kcal/mol)	$-T\Delta S$ (kcal/mol)	ΔG (kcal/mol)
1G3	−1689.84 ± 92.54	5.58	−1684.26 ± 92.54
1G4	−3672.99 ± 225.05	9.35	−3663.64 ± 225.05
2G3	−3570.95 ± 191.76	−19.41	−3590.36 ± 191.76
2G4	−6880.43 ± 373.4	39.8	−6840.63 ± 373.4
1G3−10 mM	−479.5 ± 28.53	11.52	−467.98 ± 28.53
1G3−150 mM	−198.43 ± 7.68	3.11	−195.32 ± 7.68
1G4−10 mM	−3465.36 ± 192.27	9.02	−3456.34 ± 192.27
1G4−150 mM	−2206.73 ± 110.19	8.24	−2198.49 ± 110.19

For the case of 1G3 the entropy per Na^+ ion is 9.5 cal/(mol K) which can be compared to the entropy of 9.0 cal/(mol K) per Na^+ ion when only siRNA is present. In this case we find the gain in entropy per Na^+ ion is 0.5 cal/(mol K) which helps in the complexation (see Table 2). For the case of 1G4 also, we find the gain in entropy per Na^+ ion to be 0.8 cal/(mol K) due to release from the spine of siRNA during the complexation (see Table 2). A similar gain in entropy for Na^+ is also observed for the case of 2G3 and 2G4. To our knowledge, this is the first time that a quantitative estimate of the ion entropy due to their release during the complexation has been reported. A large gain in entropy due to the release of Na^+ ions for the case of 1G4 also provide better binding free energy for the case of G4 compared to the case of G3 as shown in Table 3.

III.1.4. Number of Water Molecules in the Hydration shell of siRNA. The complexation between siRNA and dendrimer causes removal of not only Na^+ ions from the spine of siRNA but also the some of the water molecules present in the spine of hydration of siRNA. We have calculated the number of water molecules around within 3 Å of siRNA for all the cases reported in this paper and have plotted this number of water molecules as a function of simulation time in Figure 5. We see that as simulation time progresses the degree of binding/wrapping of siRNA increases and water molecules in the hydration shell of siRNA is expelled to assist this binding event. This leads to the decreases in number of water molecules in the hydration shell of siRNA. This picture is very different in the case of 2G4. The number of water molecules around siRNA for 2G4 case is approximately equal to 1G4. This change of trend is due to the special spatial arrangement of dendrimer: in the case of 2G4, two dendrimers are not able to wrap the siRNA, they just bind or stick to siRNA in the two opposite backbone faces of siRNA, and hence, the water molecules in front and back face of siRNA are not moved but more water molecules are moved from backbone sides of siRNA. In contrast, for 1G4, siRNA wraps the dendrimer, and hence, the number of water molecules around siRNA is expelled and so the number decreases.

III.2. Binding Energy and Structural Properties in Equilibrium State. *III.2.1. Binding Energy*. We have calculated the

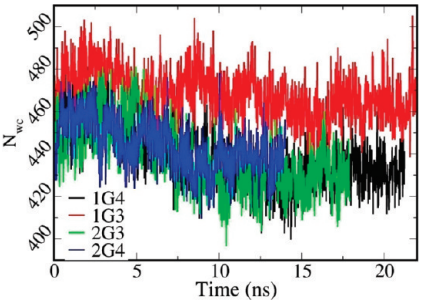

Figure 5. Variation of the number of water molecules around siRNA (any molecules within 3 Å) when it complex with dendrimer of generation 3 (1G3) and 4 (1G4) and the same generation with two dendrimers (2G3 and 2G4).

binding energy for the siRNA−dendrimer complex for all the cases using the molecular mechanics/Poisson−Boltzmann surface area method (MM−PBSA) module of AMBER9 along with the 2PT thermodynamic method for entropy calculation.[68−71] In general the binding free energy for the noncovalent association of two molecules may be written as

$$\Delta G(A + B \rightarrow AB) = G_{AB} - G_A - G_B$$

For any species on the right-hand side $G(X) = H(X) - TS(X)$, in view of this expression, the above binding energy can be written as

$$\Delta G_{bind} = \Delta H_{bind} - T\Delta S_{bind}$$

where $\Delta H_{bind} = \Delta E_{gas} + \Delta G_{sol}$, ΔH_{bind} is the change in enthalpy and is calculated by summing the gas-phase energies (ΔE_{gas}) and solvation free energies (ΔG_{sol}). Where $E_{gas} = E_{ele} + E_{vdw} + E_{int}$, here, E_{ele} is the Electrostatic energy calculated from the Coulomb potential, E_{vdw} is the nonbond van der Walls energy and E_{int} is the internal energy contribution from bonds, angles and torsions. $G_{sol} = G_{es} + G_{nes}$, where G_{es} is the electrostatic energy calculated from a Poisson−Boltzmann (PB) method and G_{nes} is the nonelectrostatic energy calculated as $\gamma \times \text{SASA} + \beta$ where γ is the surface tension parameter (γ = 0.00542 kcal/ Å^2) and SASA is the solvent-accessible surface area of the molecule. Calculating entropy using normal-mode analysis (as implemented in mm-pbsa) requires the computation of eigenvectors and eigenvalues through the diagonalization of the Hessian matrix and is computationally challenging for large number of atoms. For the entropy calculation we have used recently developed two-phase (2PT) thermodynamic model.[68−71] This method requires only the vibrational density of state function which can be determined from the Fourier transform of the velocity autocorrelation function. The entropy of the system is given by

$$S = k(\ln Q) + \beta^{-1}\left(\frac{\partial(\ln Q)}{\partial T}\right)_{N,V}$$

Here Q is the partition function of the system and it can be calculated from the partition function $q_{HO}(v)$ of a harmonic oscillator as given below

$$\ln Q = \int_0^\infty \mathrm{d}v\, s(v) \ln q_{HO}(v)$$

where s(v) is the density of state function and it is decomposed into gas phase (described in terms of a hard sphere model) component and a solid phase. This density of state

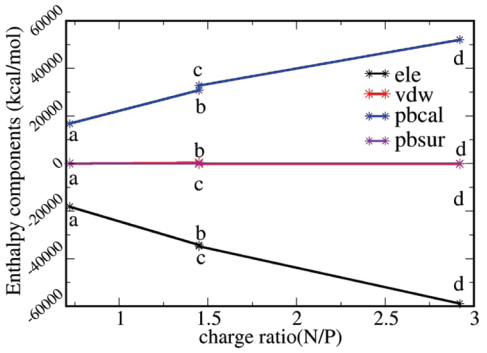

Figure 6. Various enthalpy and its components of all the cases with corresponding charge ratios. Here a, b, c, and d correspond to 1G3, 1G4, 2G3, and 2G4 complexes, respectively. Lines are guides to the eye only.

function is calculated from the Fourier transform of the velocity auto correlation function (VAC).[68]

$$S(v) = \frac{2}{kT}\sum_{j=1}^{N}\sum_{k=1}^{3} m_j \lim_{\tau \to \infty} \int_{-\tau}^{\tau} c_j^k(t) e^{-i2\pi vt}\, dt$$

where m_j is the mass of jth atom and

$$c_j^k(t) = \lim_{\tau \to \infty} \frac{1}{2\tau} \int_{-\tau}^{\tau} v_j^k(t'+t) v_j^k(t')\, dt'$$

is the velocity autocorrelation function of the jth atom in the k direction. For details of the method, we refer the readers to the original set of 2PT papers.[68−71]

The above MMPB−SA method was applied to 300 configurations from the last 3 ns of the 20 ns long MD trajectory to estimate the enthalpy of binding for all the cases. For calculating entropy using the 2PT method, we did the *NVT* simulation for 40 ps using the final restart file from the previous 20−30 ns long simulation trajectory as the input with 2 fs time step and atomic coordinates and velocities are recorded for every 4 fs. Now using the velocity coordinates the entropy of the system is calculated using the 2PT method.

Table 3 gives the details of the binding enthalpy and entropy for all the cases. For all the cases the enthalpy of binding is negative which is favorable for binding and the entropy of binding is positive except for 2G3 case which shows negative entropy change due to binding. This increase in entropy of the system after complexation for the 2G3 case is due to the larger conformational change and subsequent bending of siRNA which is clearly visible from the snapshot given in Figure 3b. The presence of one dendrimer bound to the siRNA affects the binding of the second dendrimer to siRNA. For G3, one dendrimer is not enough to wrap siRNA fully instead it wraps half of the siRNA, so in the presence of second dendrimer the both the dendrimers move in opposite direction along the backbone of siRNA due to interdendrimer repulsion. In the process, each of the dendrimers tries to wrap siRNA and causes siRNA bending.

In contrast for 2G4, none of the dendrimers are able to wrap the siRNA, and hence, siRNA behaves like a rigid substance and hence there is loss of entropy. So, among all the cases, the 2G3 complex is a better carrier for transfection and this result is in accordance with the experimental results of G3 dendrimer which shows better transfection efficiency for siRNA delivery with increased charge ratio.[37] Furthermore, we can say that the recognition between the dendrimer and siRNA is enthalpically driven by electrostatic interaction

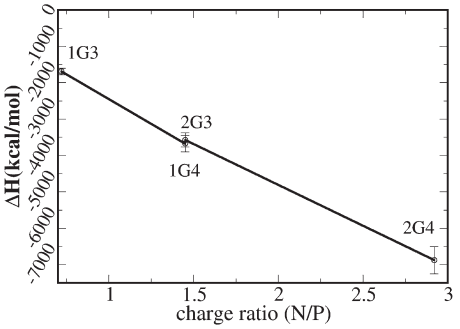

Figure 7. Enthalpy of all the cases with corresponding charge ratios. Lines are guides to the eye only.

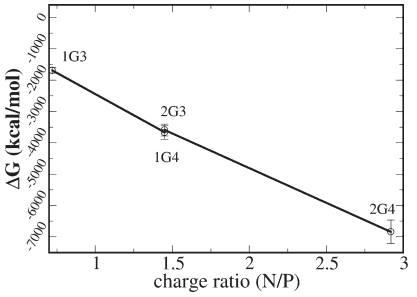

Figure 8. Binding energies of all the cases with corresponding charge ratios. Lines are guides to the eye only.

between the protonated amines in dendrimers and phosphate groups in backbone of siRNA, which one can observe from the Figure 6. Also, from Figure 6, one can observe the following interesting behavior: (i) the van der Waals interaction (vdw) and surface contribution (PBSURF) are almost constant across the charge ratio studied, (ii) the solvent electrostatic energy is increased positively as the generation and concentration of dendrimer increased, and (iii) electrostatic energy of the gas phase (solute) also increases but negatively with an increase in the generation and concentration of dendrimer. Finally, the enthalpy of the complexes increases negatively with increasing generation and concentration of dendrimer as shown in Figure 7, demonstrating the thermodynamic stability of the complex. From the above analysis, one may infer that though the electrostatic energies due to solvent phase and gas (solute) phase are increased, the contribution for negative enthalpy is coming from the electrostatic energy of gas (solute) phase only. Hence, electrostatic energy is the main contribution for binding between siRNA and dendrimer and the main cause for this interaction is the oppositely charged groups of protonated amines and phosphates presented in dendrimer and in the backbone of siRNA respectively. Change in generation and concentration of dendrimer gives charge ratio variation, and this charge ratio variation leads the change in electrostatic energy when going from one generation to other generation and for two dendrimers. From Figure 8, we see that the binding free energy follows the same trend as followed by number of contacts N_c except for the case of 2G4. Binding energy for 2G4 is higher than that of binding energy of 1G4. The larger the negative value of binding, the greater the binding affinity is between dendrimer and siRNA. We may conclude that with increases in generation and concentration of dendrimer, the charge ratio increases and hence the binding affinity is increased. The trend followed in the above results are in good accordance with the experimental results of increase in transfection and silencing when increasing the charge ratio of the complex.[36]

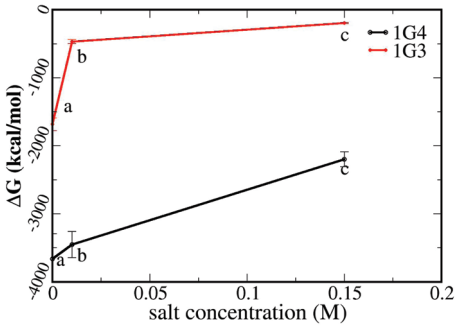

Figure 9. Binding energies of 1G3 and 1G4 with salt concentration. Here a, b and c correspond to 0 (neutral), 10, and 150 mM NaCl concentrations, respectively. Lines are guides to the eye only.

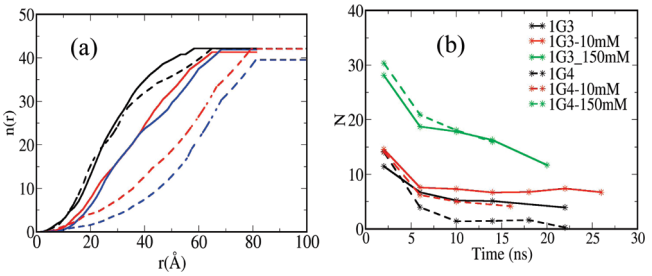

Figure 10. (a) Number of Na^+ counterions as a function of distance from the center of mass (COM) of siRNA at 2 ns (black), 6 ns (red) and 14 ns (blue). Here continuous and dotted lines correspond to 1G3 and 1G4, respectively. (b) Time variation of the number (N) of Na^+ counterions around the siRNA (within 20 Å) of 1G3 and 1G4 at two different salt concentrations. Lines are guides to the eye only.

In order to understand the effect of salt concentration on the binding affinity between siRNA and dendrimer, we have calculated the binding energy of 1G3 and 1G4 at two different salt concentrations and have plotted the same in Figure 9. We see that the binding energy decreases as salt concentration increases. This is due to the screening effect produced by counterions. As the salt concentration increases more and more counterions get condensed on siRNA leading to the screening of electrostatic interaction. The degree of counterion condensation as a function of salt concentration can be studied by calculating the counterion density around siRNA as a function of time. The counterion density (for Na^+ ions) for the charge neutral case (0 molar case) has been shown in Figure 10a for the case of 1G3 and 1G4 at various instant of time. We see that as time progresses more and more Na^+ ions are pushed away from the vicinity of siRNA releasing the condensed counterions. In the process there is gain in the counterion entropy as will be demonstrated in section III.1.3. Now while comparing the Na^+ ions density profile for the charge neutral and two different salt concentration cases we find that larger number of Na^+ ions are in the vicinity of siRNA and this number increase as the salt concentration increases as shown in Figure 10b. The degree of condensation and release of counterions as a function of salt concentration give rise to the salt dependence of binding affinity of siRNA−dendrimer complexation. In the case of 1G3, at 10 mM salt concentration negative charges on siRNA is greatly screened and hence the electrostatic interaction between the positive charges of the G3 dendrimer and siRNA is weakened. At the same molarity because of greater number of positive charges for G4 dendrimer the electrostatic interaction between siRNA and dendrimer is less affected compared to G3. However, with the further increase

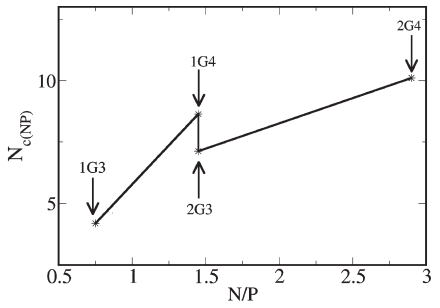

Figure 11. Average number of contacts between N and P of all the cases with corresponding charge ratios (N/P). Lines are guides to the eye only.

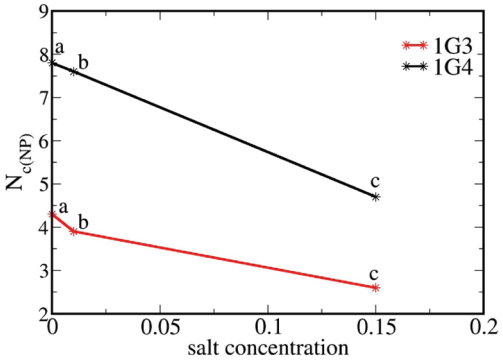

Figure 12. Average number of contacts between N and P of 1G4 and 1G3 with salt concentration. Here a, b, and c correspond to 0 (neutral), 10, and 150 mM NaCl concentrations, respectively. Lines are guides to the eye only.

in slat concentration (for example 150 mM) the binding affinity for G4 is also greatly reduced because of strong screening of electrostatic interaction which is hard to overcome even with the large number positive charges on G4.

To get a microscopic picture of the binding, we calculate the number of contacts between nitrogen in the amine group of dendrimer and the phosphate in backbone of siRNA. The results obtained are presented in the next section.

III.2.2. Contacts between N and P. We have calculated the number of contacts between the nitrogen N in the amine group of dendrimer and phosphate P in the backbone of siRNA for all the cases and averaged over last 4 ns of the production runs (14−20 ns long runs depending on the dendrimer generation). We have plotted this average number of contacts for all the cases as a function of charge ratio (N/P ratio) in Figure 11. From this figure, we observe that as charge ratio increases the contacts between N and P also increases. Because of the repulsion between two dendrimers of generation 3 for the 2G3 case the contacts between N and P for 2G3 is less than that of 1G4 case. The number of contacts gives a quantitative estimate of the binding and the interaction strength between siRNA and dendrimer. Hence, one can infer that interaction strength between siRNA and dendrimer increases as the generation increases and also the concentration of the dendrimer increases. These results and binding energy as a function of charge ratio show good agreement with the available experimental results.[36] We have also calculated the number of contacts at two different salt concentrations for the case of 1G3 and 1G4 and have plotted the same as a function of molarities in Figure 12. From this figure, we find that at low salt concentration the number of contacts between N and P for 1G4 is not affected much when compared with 1G3. In contrast at higher salt concentration the number of contacts between N and P decreases for both

1G3 and 1G4 systems because of screening effect produced by the counterions. Our calculated binding energy and number of contacts between N and P at two different salt concentrations indicate that the interaction between siRNA and dendrimer strongly depends on the salt concentration. Because of the large N/P ratio, 1G4 shows better binding affinity both in the charge neutral as well as in higher salt concentrations, compared to the 1G3 case under similar solution conditions. This led us to conclude that the interaction or binding affinity of the complexes having two dendrimers may also depend on salt concentration in a similar fashion like the case of single dendrimer. Even though the complexation of siRNA and dendrimer is affected by salt concentration, still the binding affinity mainly depends on generation of dendrimer (N/P ratio between dendrimer and siRNA) as well as the concentration of dendrimers. Thus, for the remainder of the analysis such as spatial distribution of amines, we consider the complexation at charge neutral case only (0 molarity).

III.2.3. Radial Distribution Functions. Radial distribution functions (RDF) between various groups in dendrimer and siRNA can give a microscopic picture of the binding. We have calculated the radial distribution function between various amines in dendrimer and the phosphates in backbone of siRNA using the configuration of the last 4 ns long simulations. RDF can give a physical picture as to how the amines groups are spatially arranged in space and which amines group are closer to phosphates in the backbone of siRNA. Depending on this spatial behavior of amines, one can conclude whether dendrimer of a given generation is behaving like flexible or rigid object. This can give information as to whether the dendrimer is trying to wrap siRNA along with binding or it just binds without wrapping. The plots shown in Figure 13 represent the radial distribution profiles of various amines groups in dendrimer with the phosphates in the backbone of siRNA for all the complexes studied in this paper. In order to distinguish between various amines distribution profile we have labeled amines of various subgeneration as follows: N0, N1, N2, N3, and N4 corresponding to core, first generation, second generation, third generation, and fourth generation amines, respectively. The first highest peak in all the plots in Figure 13 show that, the main contribution of binding affinity between dendrimer and siRNA comes from the terminal amines of the dendrimers. Another interesting feature from these plots is that depending on the height of the second highest peak for a given generation of amines we can infer whether the dendrimer is wrapping the siRNA or not. For example for the case of 1G3 and 1G4, the radial distribution profiles reveal that, terminal amines have highest peak followed by the next nearest highest peaks with contribution coming either from core (N0) or from first generation amines (N1) for the case of 1G4. In the case of 1G3, the second peak has contributions only from the first generation amines. For the case of 2G3 complex, we have two dendrimers, so we have calculated radial distribution function of various amines in each dendrimer separately which is shown in parts c and d of Figure 13. From these figures, we infer that, for both the dendrimers among all other amines, terminal amines have highest peak first which shows the main contribution of binding affinity between siRNA and dendrimer. Further, the second highest peak has contribution only from the first generation amines of first dendrimer in 2G3 complex (see Figure 13c or the core amines of second dendrimer in 2G3 complex (see Figure 13d). Following very interesting microscopic picture emerges from the radial distribution function for 1G3, 1G4, and 2G3: phosphates of siRNA are spatially closer to terminal amines first, and the next closer amines are

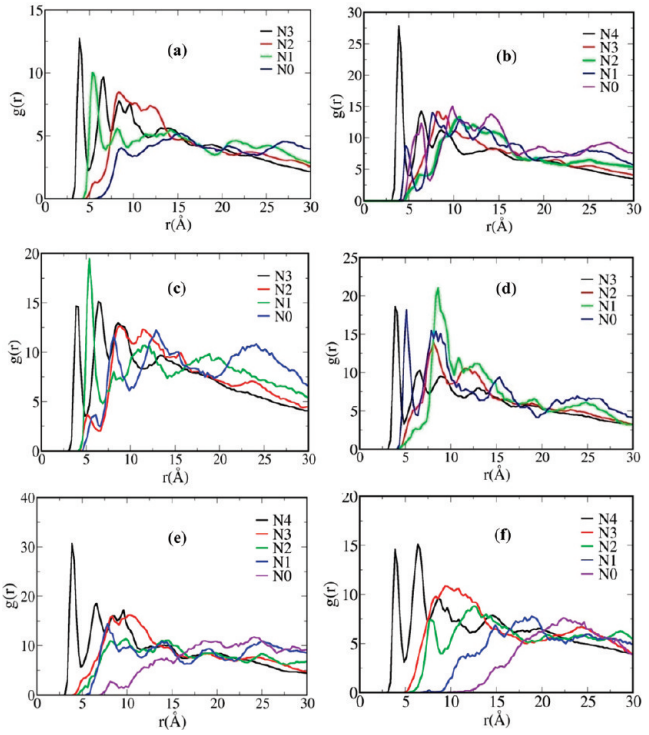

Figure 13. Radial distribution function between phosphate in siRNA and various amines in dendrimer of (a) 1G3, (b) 1G4, (c) first dendrimer of 2G3, (d) second dendrimer of 2G3, (e) first dendrimer of 2G4, and (f) second dendrimer of 2G4.

core and first generation amines, respectively. From this, one can say that dendrimers are trying to wrap the siRNA, and thus they act like a flexible substance. But for the case of 2G4, expect for the terminal amines, other amines do not show any significant binding affinity to the phosphate as is evident from the absence of a sharp peak in the radial distribution profile between amines of lower subgeneration and phosphate shown in Figure 13, parts e and f. From this, one can conclude that, the dendrimers are not wrapping the siRNA, they just bind or stick to siRNA. This is due to the repulsion between the dendrimers. So one dendrimer of generation 4 is enough for wrapping the siRNA, and if the complex has two dendrimers of generation 4, siRNA acts like a rigid substance. From this conclusion, one may think of making a bundle kind of carrier by adding more and more siRNA and dendrimers of generation 4, which can transfer more than one siRNA in a single transfection.

IV. Summary and Conclusions

To summarize, we have studied the structural behavior and energetic of the complexation of siRNA with following systems: (i) one dendrimer of generation 3 and 4 (1G3 and 1G4), (ii) two dendrimers of the same generations (2G3 and 2G4) and (iii) one dendrimer of the same generations (1G3 or 1G4) at two different salt concentrations through atomistic molecular dynamic simulations in explicit salt water. Our calculated binding energies suggest that as the dendrimer generation increases (i.e., going from G3 to G4) binding efficiency increases due to the increase in N/P charge ratio. For a given generation N/P ratio can be increased by increasing the number of dendrimer and hence binding energy also increases in going from one dendrimer to two dendrimer for a given generation (i.e., 2G3 shows better binding compared to 1G3). As the charge ratio increases number of contacts between amine groups of dendrimer and phosphate in the backbone of siRNA in other words interaction between

siRNA and dendrimer gets increased and binding energy also gets increased. From these results, we observe the following features: (i) Among G3 and G4, G4 shows higher binding affinity and hence 1G4 is a stable complex when compare with 1G3. (ii) Among 1G3 and 2G3, since charge ratio increases when we go from one dendrimer to two dendrimers, 2G3 shows better binding affinity and also 2G3 is a stable complex when compare with 1G3. (iii) Among 1G4 and 2G4, here also the charge ratio increased, so 2G4 shows better binding affinity. Furthermore, our results of 1G3 and 1G4 at two different salt concentrations show salt dependency on binding affinity between siRNA and dendrimer. The radial distribution profile of various amines in dendrimer and phosphate in backbone of siRNA tells us that, though the charge ratio is increased for 2G4 when compared with 1G4 but dendrimers in 2G4 are not able to wrap the siRNA due to the repulsion between the dendrimers. Hence, one may say that the increasing the charge ratio for stable complex is not only increasing the positives charge of carrier but one should increase siRNA concentration also. By increasing the siRNA concentration for multiple dendrimers in the case of generation 4 gives a suggestion to make a bundle kind of carrier which can carry more than one siRNA. Our results reveal that, one dendrimer of generation 4 and two dendrimers of generation 3 shows best compact complex and two dendrimer of generation 4 shows strong binding affinity. We believe that the results reported in this paper will have important consequences in the design of effective nanocarriers.

The outcomes of this paper propose new line of research to make bundle kind of carrier which may carry more than one siRNA at once. In future, we plan to investigate the stability of complex in serum and also cellular uptake of the complex through lipid membrane.

Acknowledgment. We acknowledge computational resource supported by the DST Centre for Mathematical Biology at IISc. We also thank Prof. Sriram Ramaswamy for allowing us to use his computational facility. P.K.M. thanks DST, India, for financial support.

Supporting Information Available: Figure S1, showing the rise of siRNA as a function of time for the 1G3 and 1G4 complex. This material is available free of charge via the Internet at http://pubs.acs.org.

References and Notes

(1) Meister, G.; Tuschl, T. *Nature* **2004**, *431* (7006), 343–349.
(2) Hannon, G. J.; Rossi, J. J. *Nature* **2004**, *431* (7006), 371–378.
(3) Fire, A.; Xu, S. Q.; Montgomery, M. K.; Kostas, S. A.; Driver, S. E.; Mello, C. C. *Nature* **1998**, *391* (6669), 806–811.
(4) Martinez, J.; Patkaniowska, A.; Urlaub, H.; Luhrmann, R.; Tuschl, T. *Cell* **2002**, *110*, 563–574.
(5) DeRouchey, J.; Schmidt, C.; Walker, G. F.; Koch, C.; Plank, C.; Wagner, E.; Radler, J. O. *Biomacromolecules* **2008**, *9*, 724–732.
(6) Elbashir, S. M.; Harborth, J.; Lendeckel, W.; Yalcin, A.; Weber, K.; Tuschl, T. *Nature* **2001**, *411* (6836), 494–498.
(7) Soutschek, J.; Akinc, A.; Bramlage, B.; Charisse, K.; Constien, R.; Donoghue, M.; Elbashir, S.; Geick, A.; Hadwiger, P.; Harborth, J.; John, M.; Kesavan, V.; Lavine, G.; Pandey, R. K.; Racie, T.; Rajeev, K. G.; Rohl, I.; Toudjarska, I.; Wang, G.; Wuschko, S.; Bumcrot, D.; Koteliansky, V.; Limmer, S.; Manoharan, M.; Vornlocher, H. P. *Nature* **2004**, *432* (7014), 173–178.
(8) Kim, D. H.; Rossi, J. J. *Nat. Rev. Genet.* **2007**, *8* (3), 173–184.
(9) Behlke, M. A. *Mol. Ther.* **2006**, *13*, 644–670.
(10) Aagaard, L.; Rossi, J. J. *Adv. Drug Delivery Rev.* **2007**, *59* (2−3), 75–86.
(11) Von Eije, K. J.; Aagaard, L.; Saetrom, P.; Amarzguioui, M.; Li, H. T.; Rossi, J. J. *Hum. Gene Ther.* **2007**, *18*, 1068–1068.
(12) de Fougerolles, A.; Vornlocher, H. P.; Maraganore, J.; Lieberman, J. *Nature Rev. Drug Discovery* **2007**, *6*, 443–453.
(13) Rossi, J. J. *Biotechniques* **2006**, *40*, S25–S29.
(14) Mintzer, M. A.; Simanek, E. E. *Chem. Rev.* **2009**, *109*, 259–302.
(15) Gao, K.; Huang, L. *Mol. Pharm.* **2009**, *6*, 651–658.
(16) Tsubouchi, A.; Sakakura, J.; Yagi, R.; Mazaki, Y.; Schaefer, E.; Yano, H.; Sabe, H. *J. Cell Biol.* **2002**, *159*, 673–683.
(17) Duxbury, M. S.; Ito, H.; Benoit, E.; Zinner, M. J.; Ashley, S. W.; Whang, E. E. *Biochem. Biophys. Res. Commun.* **2003**, *311*, 786–792.
(18) Grayson, A. C. R.; Doody, A. M.; Putnam, D. *Pharm. Res.* **2006**, *23*, 1868–1876.
(19) Santel, A.; Aleku, M.; Keil, O.; Endruschat, J.; Esche, V.; Durieux, B.; Loffler, K.; Fechtner, M.; Rohl, T.; Fisch, G.; Dames, S.; Arnold, W.; Giese, K.; Klippel, A.; Kaufmann, J. *Gene Ther.* **2006**, *13*, 1360–1370.
(20) Bouxsein, N. F.; McAllister, C. S.; Ewert, K. K.; Samuel, C. E.; Safinya, C. R. *Biochemistry* **2007**, *46*, 4785–4792.
(21) Palliser, D.; Chowdhury, D.; Wang, Q. Y.; Lee, S. J.; Bronson, R. T.; Knipe, D. M.; Lieberman, J. *Nature* **2006**, *439* (7072), 89–94.
(22) Liu, Z.; Winters, M.; Holodniy, M.; Dai, H. J. *Angew. Chem., Int. Ed.* **2007**, *46*, 2023–2027.
(23) Kam, N. W. S.; Liu, Z.; Dai, H. J. *J. Am. Chem. Soc.* **2005**, *127*, 12492–12493.
(24) Podesta, J. E.; Al-Jamal, K. T.; Herrero, M. A.; Tian, B. W.; Ali-Boucetta, H.; Hegde, V.; Bianco, A.; Prato, M.; Kostarelos, K. *Small* **2009**, *5*, 1176–1185.
(25) Simeoni, F.; Morris, M. C.; Heitz, F.; Divita, G. *Nucleic Acids Res.* **2003**, *31*, 2717–2724.
(26) Muratovska, A.; Eccles, M. R. *FEBS Lett.* **2004**, *558* (1−3), 63–68.
(27) Chiu, Y. L.; Ali, A.; Chu, C. Y.; Cao, H.; Rana, T. M. *Chem. Biol.* **2004**, *11*, 1165–1175.
(28) Minakuchi, Y.; Takeshita, F.; Kosaka, N.; Sasaki, H.; Yamamoto, Y.; Kouno, M.; Honma, K.; Nagahara, S.; Hanai, K.; Sano, A.; Kato, T.; Terada, M.; Ochiya, T. *Nucleic Acids Res.* **2004**, *32* (13), e109/1–e109/7.
(29) Puebla, I.; Esseghir, S.; Mortlock, A.; Brown, A.; Crisanti, A.; Low, W. *J. Biotechnol.* **2003**, *105* (3), 215–226.
(30) Takei, Y.; Kadomatsu, K.; Yuzawa, Y.; Matsuo, S.; Muramatsu, T. *Cancer Res.* **2004**, *64*, 3365–3370.
(31) Rolland, O.; Turrin, C. O.; Caminade, A. M.; Majoral, J. P. *New J. Chem.* **2009**, *33*, 1809–1824.
(32) Astruc, D.; Boisselier, E.; Ornelas, C. *Chem. Rev.* **2010**, *110*, 1857–1959.
(33) KukowskaLatallo, J. F.; Bielinska, A. U.; Johnson, J.; Spindler, R.; Tomalia, D. A.; Baker, J. R. *Proc. Natl. Acad. Sci. U.S.A.* **1996**, *93*, 4897–4902.
(34) Kihara, F.; Arima, H.; Tsutsumi, T.; Hirayama, F.; Uekama, K. *Bioconjugate Chem.* **2003**, *14*, 342–350.
(35) Kihara, F.; Arima, H.; Tsutsumi, T.; Hirayama, F.; Uekama, K. *Bioconjugate Chem.* **2002**, *13*, 1211–1219.
(36) Zhou, J. H.; Wu, J. Y.; Hafdi, N.; Behr, J. P.; Erbacher, P.; Peng, L. *Chem. Commun.* **2006**, 2362–2364.
(37) Tsutsumi, T.; Hirayama, F.; Uekama, K.; Arima, H. *J. Controlled Release* **2007**, *119*, 349–359.
(38) Waite, C. L.; Sparks, S. M.; Uhrich, K. E.; Roth, C. M. *BMC Biotechnol.* **2009**, *9*, 38/1–38/10.
(39) Agrawal, A.; Min, D. H.; Singh, N.; Zhu, H. H.; Birjiniuk, A.; von Maltzahn, G.; Harris, T. J.; Xing, D. Y.; Woolfenden, S. D.; Sharp, P. A.; Charest, A.; Bhatia, S. *ACS Nano* **2009**, *3*, 2495–2504.
(40) Pavan, G. M.; Posocco, P.; Tagliabue, A.; Maly, M.; Malek, A.; Danani, A.; Ragg, E.; Catapano, C. V.; Pricl, S. *Chem. Eur. J.* **2010**, *16*, 7781–7795.
(41) Waite, C. L.; Roth, C. M. *Bioconjugate Chem.* **2009**, *20*, 1908–1916.
(42) Patil, M. L.; Zhang, M.; Betigeri, S.; Taratula, O.; He, H.; Minko, T. *Bioconjugate Chem.* **2008**, *19*, 1396–1403.
(43) Pavan, G. M.; Danani, A.; Pricl, S.; Smith, D. K. *J. Am. Chem. Soc.* **2009**, *131*, 9686–9694.
(44) Larin, S. V.; Darinskii, A. A.; Lyulin, A. V.; Lyulin, S. V. *J. Phys. Chem. B* **2010**, *114*, 2910–2919.
(45) Lyulin, S. V.; Darinskii, A. A.; Lyulin, A. V. *Macromolecules* **2005**, *38*, 3990–3998.
(46) Lyulin, S. V.; Vattulainen, I.; Gurtovenko, A. A. *Macromolecules* **2008**, *41*, 4961–4968.
(47) Larin, S.; Lyulin, S.; Lyulin, A.; Darinskii, A. *Macromol. Symp.* **2009**, *278*, 40–47.
(48) Maiti, P. K.; Bagchi, B. *Nano Lett.* **2006**, *6*, 2478–2485.
(49) Pavan, G. M.; Albertazzi, L.; Danani, A. *J. Phys. Chem. B* **2010**, *114*, 2667–2675.
(50) Orberg, M. L.; Schillen, K.; Nylander, T. *Biomacromolecules* **2007**, *8*, 1557–1563.

(51) Case, D. A.; Darden, T. A.; Cheatham, T. E. I.; Simmerling, C. L.; Wang, J.; Duke, R. E.; Luo, R.; Merz, K. M.; Pearlman, D. A.; Crowley, M.; Walker, R. C.; Zhang, W.; Wang, B.; Hayik, S.; Roitberg, A.; Seabra, G.; Wong, K. F.; Paesani, F.; Wu, X.; Brozell, S.; Tsui, V.; Gohlke, H.; Yang, L.; Tan, C.; Mongan, J.; Hornak, V.; Cui, G.; Beroza, P.; Mathews, D. H.; Schafmeister, C.; Ross, W. S.; Kollman, P. A. *AMBER version 9.0*; University of California: San Francisco, CA, 2006.
(52) Cornell, W. D.; Cieplak, P.; Bayly, C. I.; Gould, I. R.; Merz, K. M.; Ferguson, D. M.; Spellmeyer, D. C.; Fox, T.; Caldwell, J. W.; Kollman, P. A. *J. Am. Chem. Soc.* **1995**, *117*, 5179–5197.
(53) Mayo, S. L.; Olafson, B. D.; Goddard, W. A. *J. Phys. Chem.* **1990**, *94*, 8897–8909.
(54) (a) Maiti, P. K.; Cagin, T.; Wang, G. F.; Goddard, W. A. *Macromolecules* **2004**, *37*, 6236–6254. (b) Maiti, P. K.; Cagin, T.; Lin, S. T.; Goddard, W. A. *Macromolecules* **2005**, *38*, 979–991. (c) Maiti, P. K.; Messina, R. *Macromolecules* **2008**, *41*, 5002–5006. (d) Maiti, P. K.; Li, Y.; Cagin, T.; Goddard, W. A. *J. Chem. Phys.* **2009**, *130*, 144902/1–144902/10. (e) Maiti, P. K.; Bagchi, B. *J. Chem. Phys.* **2009**, *131*, 214901/1–214901/7.
(55) Yuan, Y. R.; Pei, Y.; Chen, H. Y.; Tuschl, T.; Patel, D. J. *Structure* **2006**, *14*, 1557–1565.
(56) Ryckaert, J. P.; Ciccotti, G.; Berendsen, H. J. C. *J. Comput. Phys.* **1977**, *23*, 327–341.
(57) Berendsen, H. J. C.; Postma, J. P. M.; Vangunsteren, W. F.; Dinola, A.; Haak, J. R. *J. Chem. Phys.* **1984**, *81* (8), 3684–3690.
(58) Maiti, P. K.; Pascal, T. A.; Vaidehi, N.; Goddard, W. A. *Nucleic Acids Res.* **2004**, *32* (20), 6047–6056.
(59) Overbeek, J. T.; Voorn, M. J. *J. Cell. Comp. Physiol.* **1957**, *49*, 7–26.
(60) Nakajima, A.; Sato, H. *Biopolymers* **1972**, *11*, 1345–1355.
(61) Castelnovo, M.; Joanny, J. F. *Eur. Phys. J. E* **2001**, *6*, 377–386.
(62) Ou, Z. Y.; Muthukumar, M. *J. Chem. Phys.* **2006**, *124*, 154902/1–154902/11.
(63) Kramarenko, E. Y.; Khokhlov, A. R. *Polym. Sci., Series A* **2007**, *49*, 1053–1063.
(64) Kegler, K.; Salomo, M.; Kremer, F. *Phys. Rev. Lett.* **2007**, *98*, 058304/1–058304/4.
(65) Spruijt, E.; Stuart, M. A. C.; van der Gucht, J. *Macromolecules* **2010**, *43*, 1543–1550.
(66) Spruijt, E.; Sprakel, J.; Stuart, M. A. C.; van der Gucht, J. *Soft Matter* **2010**, *6* (1), 172–178.
(67) Messina, R. *J. Phys.: Condens. Matter* **2009**, *21*, 113102/1–113102/18.
(68) Lin, S. T.; Blanco, M.; Goddard, W. A. *J. Chem. Phys.* **2003**, *119*, 11792–11805.
(69) Lin, S. T.; Maiti, P. K.; Goddard, W. A. *J. Phys. Chem. B* **2005**, *109*, 8663–8672.
(70) Jana, B.; Pal, S.; Maiti, P. K.; Lin, S. T.; Hynes, J. T.; Bagchi, B. *J. Phys. Chem. B* **2006**, *110*, 19611–19618.
(71) Lin, S. T.; Maiti, P. K.; Goddard, W. A. *J. Phys. Chem. B* **2010**, *114*, 8191–8198.